

Genuine localisation transition in a long-range hopping model

Xiangyu Cao and Alberto Rosso
LPTMS, CNRS, Univ. Paris-Sud, Université Paris-Saclay, 91405 Orsay, France

Jean-Philippe Bouchaud
Capital Fund Management, 23 rue de l'Université, 75 007 Paris, France

Pierre Le Doussal
CNRS-Laboratoire de Physique Théorique de l'École Normale Supérieure, 24 rue Lhomond, 75231 Paris Cedex, France

We introduce and study a new Banded Random Matrix model describing sparse, long range quantum hopping in one dimension. Using a series of analytic arguments, numerical simulations, and a mapping to a long range epidemics model, we establish the phase diagram of the model. A genuine localisation transition, with well defined mobility edges, appears as the hopping rate decreases slower than ℓ^{-2} , where ℓ is the distance. Correspondingly, the decay of the localised states evolves from a standard exponential shape to a stretched exponential and finally to a novel $\exp(-C \ln^\kappa \ell)$ behaviour, with $\kappa > 1$.

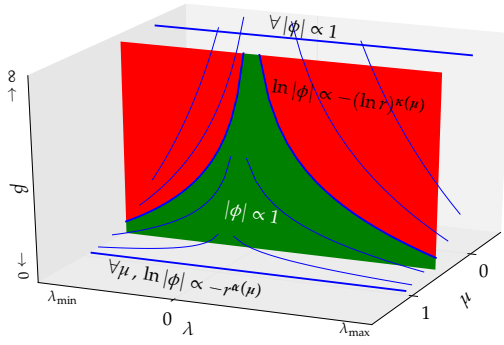


Figure 1. Schematic phase diagram of BBRMs. In the regime $\mu \in (0, 1)$, there is a mobility edge $\lambda(\beta; \mu)$ (blue curves) separating localised eigenstates (red region) and extended eigenstates (green region). The localised states have a very peculiar decay, Eq. (7). When $\mu > 1$, all the eigenstates are localised, but with a stretched exponential decay for $\mu < 2$, Eq. (10).

Since the premonitory work of Anderson [1], the existence of localisation transition (LT) of eigenstates of random Hamiltonians is a fundamental and non-trivial problem. It was settled for the single-particle Anderson model in d -dimension only much later [2]. When $d > 2$ the LT exists and manifests itself as *mobility edges* in the eigenvalue spectrum, that separate extended and localised eigenstates in the spectrum. At the vicinity of mobility edge, the eigenstates have multi-fractal statistics, described by a LT critical point. When $d \leq 2$, on the other hand, all eigenstates are localised (for the standard Anderson model) and there is no mobility edge. There has been a renewed surge of interest on these issues in the context of many-body localisation (see *e.g.* [3–5]), with intriguing suggestions of the possibility of extended, but non ergodic quantum states.

In this respect, 1-d random Hamiltonians with long-range hopping are important laboratories to understand

LTs, as they can be seen as proxies for higher dimension models. The best-known such model is the Power-law Random Banded Matrix (PBRM) ensemble [6]. Its elements H_{nm} are independent centered Gaussian random variables such that [7]

$$\overline{H_{nm}^2}^c = \frac{1}{1 + g_{nm}}; \quad g_{nm} := \beta |n - m|^{1+\mu}, \quad (1)$$

where $\beta, \mu > 0$ are some coefficients. The PBRM phase diagram can be qualitatively understood by comparing the typical nearest level spacing $\sim 1/N$ (where N is the size of the matrix) with the *direct* hopping element $\gtrsim 1/N^{1+\mu}$. When $\mu < 1$, all the eigenstates are extended; when $\mu > 1$, they are all localised but with power-law decay [6]. Remarkably, at $\mu = 1$, there is a line of critical models (parametrised by β) with multi-fractal eigenstates, which were studied numerically [8] and analytically [9, 10] (see [11] for a review, and [12] for recent work). Yet, there is no mobility edge in this case, making this transition qualitatively different from the conventional LT. The phase diagram is oversimplified because *direct* tunneling dominates transport in the quantum *small world* that PBRM describes. In fact, the above picture applies whenever the entry distributions are of the form $P(H) = \sqrt{g} P_0(\sqrt{g}H)$ for $g \rightarrow \infty$, where P_0 is “narrow” such that the moments obey $\overline{H^p} \propto g^{-p/2}$ in the large g limit. This means that all matrix elements corresponding to a certain (large) distance $|n - m|$ have the same order of magnitude.

In this Letter, we define new class of Banded Random Matrices, where the elements Q_{nm} are *sparse*. We argue that a genuine LT with a mobility edge exists in this case. More precisely, we choose the distribution of Q 's such that its positive moments are governed by small fraction ($O(1/g)$ with $g \sim |n - m|^{1+\mu} \rightarrow \infty$) of large elements, while all the other elements are very small. This implies that the moments of Q behave as $\overline{Q^p} \propto g^{-1}, \forall p$. We will in fact study a concrete model, the *Beta Banded Random Matrix* (BBRM) ensemble, inspired by a recently intro-

duced long range epidemics model [13, 14]. A BBRM is defined as a real symmetric $N \times N$ matrix whose diagonal entries are all zero ($Q_{nn} \equiv 0$) and all off-diagonal entries Q_{nm} are independent random variables in $(0, 1)$, distributed according to the following special case of Beta distribution [15]:

$$\mathbb{P}(Q < q \in (0, 1)) = q^{\frac{1}{g}}. \quad (2)$$

Equivalently, $Q_{nm} = e^{-\beta\tau_{nm}}$ where τ_{nm} are exponentially distributed with mean $|n - m|^{1+\mu}$. The moments of Q are given by $\overline{Q^p} = 1/(1 + pg)$. Note in particular that the second moment (and variance) of Q has exactly the same asymptotic decay as for the PBRM, Eq. (1). However, the typical value of Q is exponentially small in g , whereas the typical value of H is of order $g^{-1/2}$. Hence, as shown in [15], Fig. 1, the magnitude of Q_{nm} has much broader fluctuations than those of $|H_{nm}|$. This broad distribution of matrix elements makes the BBRM akin to Lévy matrices [16]. Although there are important differences between the two models (for example, the former has a bounded density of states, see below, while the latter has power-law tails extending to infinity), a LT with a mobility edge exists in both ensembles [5, 16].

Due to the absence of diagonal disorder, the BBRM's density of states (DoS) $\rho(\lambda)$ is in fact quite peculiar: see [15], Fig. 1. It develops a divergence at $\lambda = 0$, and a non-analyticity at $\lambda = \pm 1$ as β increases. For $\beta \gg 1$, most elements are vanishing, and a crude estimate of DoS is given by the distribution of the eigenvalues $\pm Q_{01}$ of the 2×2 sub-matrix $\begin{pmatrix} 0 & Q_{01} \\ Q_{01} & 0 \end{pmatrix}$. This leads to:

$$\rho(\lambda) \approx |\lambda|^{-1+1/\beta} / (2\beta), \text{ if } |\lambda| < 1 \quad (3)$$

and $\rho(\lambda) \approx 0$ for $|\lambda| > 1$. For a comparison, the PBRM DoS is always given by Wigner's semi-circle law [17].

Localisation of the eigenstates – As we have seen, the BBRM elements are typically much smaller than those of the PBRM, while sharing the same second moment. This immediately suggests that for $\mu > 1$, all states are localised for the BBRM as for the PBRM, although as we will see later the decay of the eigenstates are different in the two cases (stretched exponential vs. power law). When $\mu < 1$, the eigenstates of the PBRM are always extended while there exists a mobility edge in the BBRM case, as we argue below. Our results are qualitatively summarized in Fig. 1.

Our first argument is model-specific and works in the $\beta \rightarrow \infty$ limit. In that limit, the off-diagonal entries are vanishingly small, but so are the typical energy difference $\delta \sim \rho(\lambda)^{-1} \sim 2\beta|\lambda|^{1-1/\beta}$ near $\lambda = 0$, see Eq. (3). To compare them, let us set $\lambda = e^{-\beta\tau}$ ($\tau > 0$) and recall $Q_{nm} = e^{-\beta\tau_{nm}}$, then as $\beta \rightarrow \infty$, the ratio $\ln(Q_{nm}/\delta) \approx \beta(\tau - \tau_{nm}) \rightarrow \pm\infty$ if $\tau \gtrless \tau_{nm}$, hence the support of eigenstates can be identified with the connected components of the resonance graph formed by bonds for which $\tau > \tau_{nm}$. By Eq. (2), sites n and m are connected with

probability $P_{nm} = 1 - e^{-\tau/|n-m|^{1+\mu}} \sim \tau/|n-m|^{1+\mu}$ at large distances, and independently of other pairs. Therefore, the resonance graph defines a *long-range percolation* problem [18]. When $\tau = 0$ (resp $\tau = \infty$) the graph is completely disconnected (resp. connected). In the limit of large systems, a sharp percolation transition is expected at some τ_c , separating the insulating phase ($\tau < \tau_c$) and the percolating ($\tau > \tau_c$) phase. Indeed, a necessary criterion for the existence of the percolating phase at finite τ is the presence of a bond crossing any site i of the system. This probability is given by $p_i = 1 - \prod_{n < i} \prod_{m > i} (1 - P_{nm}) = 1 - \exp(-\tau \sum_{\ell > 0} \ell^{-\mu})$ for $\beta \gg 1$, where $\ell = n - m$. When $\mu > 1$, the sum over ℓ is convergent and $p_i < 1$, i.e. percolation is impossible and all eigenstates are localised. When $\mu < 1$, on the other hand, $p_i = 1$, and a percolation transition can occur; its existence was indeed proven in Refs. [19, 20]. So we expect a LT with mobility edges $\lambda_c \approx \pm e^{-\beta\tau_c}$ as $\beta \rightarrow \infty$. However, this estimation neglects destructive quantum interference can induce localisation in the percolation phase, so for any β finite, we have rather an upper bound $|\lambda_c| \leq \exp(-\beta\tau_c)$.

To further study the LT predicted to occur for $\mu < 1$, we now propose an approximate iterative block-diagonalisation procedure, based on an hierarchy of lengths $\ell_0 \ll \ell_1 \ll \ell_2 \ll \dots$ defined self-consistently below. At step k , we divide Q_{nm} into blocks of size $\ell_k \times \ell_k$ and let $|\phi_\alpha^{(k)}\rangle$ be the eigenstates of the matrix of diagonal blocks. In that basis, the transformed matrix elements are

$$\tilde{Q}_{\alpha\gamma}^{(k)} = \sum_{(n,m)} \langle \phi_\alpha^{(k)} | n \rangle Q_{nm} \langle m | \phi_\gamma^{(k)} \rangle. \quad (4)$$

Since the support of $\phi_\alpha^{(k)}$ is at most ℓ_k sites, the above sum contains $M_k \sim \ell_k^2$ independent elements Q_{nm} of identical distribution, weighted by random (signed) coefficients of order of magnitude := c_k . There are two cases: (i) either $|\phi_\alpha^{(k)}\rangle$ is extended and $c_k \sim (1/\sqrt{\ell_k})^2$; (ii) or it is localised around a certain site n_α , and we then assume that for $|n - n_\alpha| \sim \ell_k$, $\langle \phi_\alpha^{(k)} | n \rangle \sim e^{-a_k}$, where the decay rate a_k will be determined later, leading to $c_k \sim e^{-2a_k}$. We then define ℓ_{k+1} as the length scale such that the transformed element $\tilde{Q}_{\alpha\gamma}^{(k)}$ becomes self-averaging. It is determined by requiring that at least one atypically large $Q_{nm} \sim O(1)$ has appeared in the block, and dominates the sum (4), leading to $\tilde{Q}_{\alpha\gamma}^{(k)} \sim c_k$ (see [15] for more detailed discussion). Since the probability of an order unity element to appear on scale $|n - m| \sim \ell_{k+1}$ is $1/g_{k+1}$ with $g_{k+1} = \beta\ell_{k+1}^{1+\mu}$, self-averaging occurs when $M_k/g_{k+1} \sim 1$, or else:

$$\ln(\ell_k/\xi) = \left(\frac{2}{1+\mu} \right)^k \ln(\ell_0/\xi), \quad \xi := \beta^{\frac{1}{1-\mu}} \quad (5)$$

Note that ℓ_k is an increasing series if and only if $\mu < 1$ and $\ell_0 > \xi$. The length ξ should be compared with the microscopic scale ℓ_0 that we set such that all the matrix

elements are $\sim O(1)$; this sets $\ell_0 = \beta^{-\frac{1}{1+\mu}}$ (see Eq. (2)). For $\beta \ll 1$, one finds $\ell_0 \gg \xi$, and the iteration starts with $|\phi_\alpha^{(0)}\rangle$ which are extended. Inductively, if $|\phi_\alpha^{(k)}\rangle \sim \ell_k^{-1/2}$ is extended over ℓ_k , then $\tilde{Q}_{\alpha\gamma}^{(k)} \sim c_k = 1/\ell_k$ is larger than the typical level spacing on scale $k+1$, $\delta_{k+1} \propto \ell_{k+1}^{-1}$. Therefore the eigenstates of the diagonal blocks of size ℓ_{k+1} are still extended. Repeating this procedure *ad infinitum* we conclude the eigenstates are extended.

If now $\beta \gg 1$, the eigenstates will be localised to begin with and remain such during the iteration. We conclude that there is some β_c below which the eigenstates are extended and above which they are localised. To prove the existence of a mobility edge, β_c should depend on λ so that for a fixed β it exists $\lambda_c(\beta)$ separating extended and localised eigenstates. In fact, although Eq. (5) does not depend on λ , we now argue that the mobility edge exists because the level spacing in the above argument ($\propto 1/\rho(\lambda)$) is small when $\lambda \approx 0$ and large when λ is large.

The above framework also predicts the decay rate of the eigenstates in the localised phase. We first determine $\langle \phi_\alpha^{(k+1)} | n \rangle \sim \exp(-a_{k+1})$ as a function of $\langle \phi_\alpha^{(k)} | n \rangle \sim \exp(-a_k)$. At first order in perturbation, $\langle \phi_\alpha^{(k+1)} | n \rangle \sim \tilde{Q}_{\alpha\gamma_n}^{(k)} / \delta_k$, where γ_n is the state localised around n . Assuming faster-than-algebraic decay of the eigenstates, *i.e.* $a_k \gg \ln(\ell_k)$, we can neglect the level spacing δ_k for large k , simply leading to $\tilde{Q}_{\alpha\gamma_n}^{(k)} \sim \exp(-2a_k)$, or $a_{k+1} = 2a_k \Rightarrow a_k = 2^k a_0$. To calculate how a_k grows with ℓ_k , we use Eq. (5) to obtain:

$$a_k \propto \ln^{\kappa(\mu)}(\ell_k/\xi), \quad \kappa(\mu) = \frac{\ln 2}{\ln \frac{2}{1+\mu}}. \quad (6)$$

We conclude that the localised eigenstates decay extremely slowly, as

$$-\ln |\langle n | \phi_m \rangle| = C \ln^{\kappa(\mu)}(|n - m|/\xi), \quad (7)$$

where C is a numerical constant. Note that $\kappa(\mu) > 1$ when $\mu \in (0, 1)$, so (7) is still faster than algebraic, justifying the above faster-than-algebraic decay assumption. When $-1 < \mu < 0$, on the other hand, the LT disappears and all states are extended.

The exponent $\kappa(\mu)$ in fact already appeared in other contexts, *i.e.* long-range percolation [21, 22] and recently a long-range epidemics model [13, 14], which turn out to be intimately related to our model. The epidemics model works as follows: at initial time, only one site 0 is infected; the waiting time for a direct infection from 0 to m , τ_{0m} , is exponentially distributed with mean $\overline{\tau_{0m}} = |m|^{1+\mu}$. Infected sites wait some time $-\tau \geq 0$ and then go on to infect others. How long does it take to infect a remote site n , knowing that site 0 started the infection? This *first-passage time* is given by:

$$T_n(\tau) \stackrel{\text{def}}{=} \min_{\mathbf{p}: 0 \rightarrow n} \sum_{i=1}^s (\tau_{m_i, m_{i-1}} - \tau), \quad (8)$$

where we consider all the paths $\mathbf{p} = (m_0 = 0, m_1, \dots, m_s = n)$ connecting 0 and n and select the one with the minimum total time cost. One of the key results of [13, 14] is precisely that $T_n(0) \sim C \ln^{\kappa(\mu)}(|n|)$ if $\mu < 1$, with κ precisely given by Eq.(6). Now, a BBRM is by definition a matrix of Boltzmann factors $Q_{nm} = e^{-\beta \tau_{nm}}$. This allows us to adapt the well-known mapping between strong disorder localisation and statistical physics (see [15], Sect D), and relate the decay of localised eigenstates (*i.e.* the resolvent of Q) to the growth of $T_n(\tau)$ in the $\beta \rightarrow \infty$ limit:

$$-\ln |\langle 0 | (\lambda \mathbf{I} - \mathbf{Q})^{-1} | n \rangle| \stackrel{\beta \gg 1}{\approx} \beta T_n(0), \quad (9)$$

This identification holds provided $\lambda = e^{-\beta \tau}$ is not exponentially close to 0 as $\beta \rightarrow \infty$. In view of this relation, Eq. (7) appears as a generalisation to $\beta < \infty$ of the result $a_n(0) \propto \ln^{\kappa(\mu)} |n|$ of [13, 14] for $\mu \in (0, 1)$. Moreover, the relation Eq. (9) allows us to predict the eigenstate decay in the localised regime $\mu > 1$. Indeed, it is known that $a_n \propto |n|^{\min(2, \mu)-1}$. Hence, we expect that all the eigenstates for $\mu > 1$ have exponential or stretched exponential decay at any disorder:

$$-\ln |\langle n | \phi_0 \rangle| \sim C |n|^{\min(\mu, 2)-1}, \quad \mu > 1. \quad (10)$$

When $\mu \geq 2$ our model behaves as a short-range 1d disordered metal. In the regime $\mu \in (1, 2)$, we predict an “anomalous insulator”, with a stretched exponential localisation becoming $\exp(-\ln^\kappa n)$ for $\mu < 1$. This can be compared with the PBRM model where eigenstates are algebraically localised [6]. For $\mu = 1$, Eq. (9) and [14] predict a peculiar decay $-\ln |\langle n | \phi_0 \rangle| \sim \exp(C\sqrt{\ln n})$.

Numerics— We first study the $\mu > 1$ regime. For this we diagonalise BBRMs of size $N \times N$, and retain $N/2$ eigenstates at the center of the spectrum of each realisation. For each eigenstate $|\phi\rangle$, we define its “center” n_{\max} as the site with maximum amplitude $|\langle \phi | n \rangle|$. We then make histograms of $\ln |\langle \phi | n_{\max} \rangle / \langle \phi | n \rangle|$ as a function of $|n - n_{\max}|$. Fig. 2 shows the median of the empirical distributions. Even at a weak disorder, $\beta = 0.25$, the results compare well with the predicted stretched exponential decay, Eq. (10).

Next, we present some numerical evidence of the localisation transition predicted in the $\mu \in (0, 1)$ regime. First we study the level statistics by measuring the gap ratio [23]. Denoting $\lambda_1 \leq \dots \leq \lambda_N$ the ordered eigenvalues of a matrix, and $\delta_i = \lambda_{i+1} - \lambda_i$ the level spacings (gaps), the distribution of the ratios between neighboring gaps $r_i = \min(\delta_i, \delta_{i+1}) / \max(\delta_i, \delta_{i+1})$ satisfies $\bar{r} = r_P \approx 0.39$ in the localised phase (r_P comes from Poisson level statistics), while in the extended phase, $\bar{r} = r_{GOE} \approx 0.53$ (r_{GOE} is the numerical value for the GOE ensemble). For convenience, we define the rescaled gap ratio

$$\chi := \frac{\bar{r} - r_P}{r_{GOE} - r_P} \Rightarrow \chi \rightarrow \begin{cases} 0 & (\text{localised}), \\ 1 & (\text{delocalised}). \end{cases} \quad (11)$$

The average \bar{r} is computed over both realisations and gaps r_i for which λ_i belongs to bins of width ~ 0.2 . The

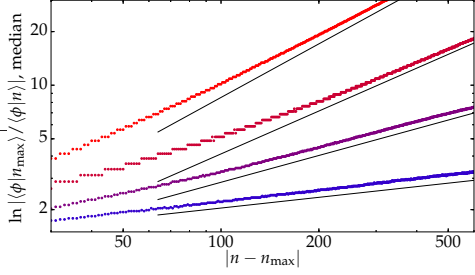


Figure 2. (Stretched) exponential decay of the localised states of $\mu = 2.5, 1.8, 1.5, 1.2$ (from top to bottom). Exact diagonalisation results (points, $N = 2^{11}$, $\beta = 0.25$, 10^4 eigenstates) are compared with the prediction Eq. (10), lines).

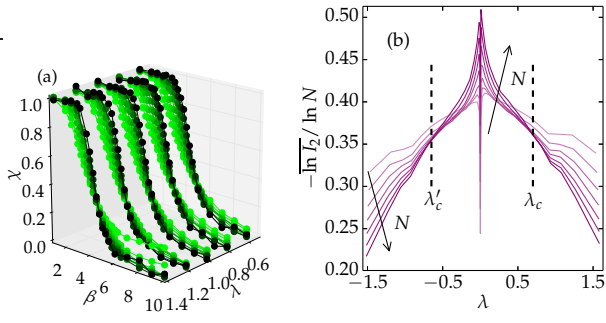


Figure 3. (a) Numerical measure of ratio χ , Eq. (11) for the BBRM model with $\mu = 0.5$, $\beta \in (1, 10)$ and of sizes $N = 2^7$ (light color) to 2^{14} (dark color). Eigenvalues in $(0.5, 1.5)$ are binned into 5 bins of equal width. More than 10^5 different gaps are averaged over for each data point. (b) Measure of the IPR of the eigenstates of BBRMs for $\mu = 0.5$, $\beta = 5$. Dashed lines indicate the mobility edges.

result, see Fig. 3, shows clear evidence for an LT: χ goes from the GOE (extended) value to the Poisson (localised) value when β increases from 1 to 10. This change becomes sharper as the system sizes increases and by zooming in [15], one observes that different curves cross at some critical value $\beta_c = \beta_c(\lambda)$, which increases as $|\lambda|$ decreases, as expected. We now turn our attention to the existence of mobility edge λ_c at fixed β , as elicited by the *inverse participation ratio* (IPR). Recall that for a normalised state ϕ ,

$$I_2 = \sum_{i=1}^N |\langle \phi | i \rangle|^4 \sim \begin{cases} O(1) & \phi \text{ localised,} \\ O(N^{-1}) & \phi \text{ extended.} \end{cases} \quad (12)$$

At the transition, $I_2 \sim N^{-q_2}$ for some $q_2(\mu) \in (0, 1)$. The IPR is a direct characterisation of the eigenstate,

and is not affected by any singularity in the DoS. Figure 3 shows the result for $\mu = 0.5$, $\beta = 5$. We observe a clear mobility edge separating extended states in the middle of the spectrum (containing $\lambda = 0$) and localised states near the edges. The measure is repeated for several other values of β , allowing us to determine the phase diagram in the (β, λ) plane for $\mu = 0.5$. For $\beta \approx 1$, the mobility edge approaches rapidly the edge of the spectrum, and we cannot exclude the existence of a value $\beta_{\text{inf}}(\mu)$ such that all eigenstates are extended when $\beta < \beta_{\text{inf}}$. Other values of μ have also been studied, and we observe that mobility edge continue to exist up to the marginal case $\mu = 1$. From a long-range percolation point of view, this is not surprising, although the $\mu = 1$ percolation transition is very peculiar in this case [19].

In this work, we have characterised the localisation properties of a particular model of Banded Random Matrices which maps exactly to a long-range epidemic model, for which several results have recently been obtained. We believe however that our results apply to any banded random matrix with broadly distributed elements, such that all positive moments Q_{mn}^p scale at large distances as $1/|n - m|^{1+\mu}$:

$$\overline{Q_{mn}^p} \sim \frac{c(p)}{\beta |n - m|^{1+\mu}}, \quad n - m \rightarrow \infty, \quad (13)$$

An example is the randomised sparse matrices associated to long range percolation [24, 25]. This universality is expected from our the “renormalisation” analysis, which requires Eq. (13) as essentially only input [15].

Although other 1d long-range matrix models are known to exhibit mobility edges, *e.g.*, the one with *non-random* hopping [26], and the Lévy matrices [5, 16], the originality of our BBRM model is that it retains a non-trivial spatial structure which is completely lost in these other models. The spatial structure of the eigenstates can therefore be meaningfully discussed within our BBRM model, which in a sense [15] interpolates between finite-dimension and Bethe-lattice [4] / random-regular-graph [27] Anderson models. Regarding the recent debate on the possible existence of a non-ergodic extended phase, the slowly decaying, barely integrable localised states found for $\mu \rightarrow 0$ in BBRMs provide an interesting scenario.

Acknowledgements. We thank G. Biroli, A. De Luca, F. Franchini, O. Giraud, A. Ludwig, C. Monthus, M. Ortúñoz, I. Rodriguez-Arias, C. Texier and T. Thiery for useful discussions. This work is supported by “Investissements d’Avenir” LabEx PALM (ANR-10-LABX-0039-PALM). We thank the hospitality of KITP (under Grant No. NSF PHY11-25915), where this work was initiated.

[1] P. W. Anderson, Phys. Rev. **109**, 1492 (1958).

[2] E. Abrahams, P. W. Anderson, D. C. Licciardello, and

T. V. Ramakrishnan, Phys. Rev. Lett. **42**, 673 (1979).

[3] R. Nandkishore and D. A. Huse, Annu. Rev. Condens. Matter Phys. **6**, 15 (2015).

[4] A. De Luca, B. L. Altshuler, V. E. Kravtsov, and A. Scardicchio, Phys. Rev. Lett. **113**, 046806 (2014).

[5] E. Tarquini, G. Biroli, and M. Tarzia, Phys. Rev. Lett. **116**, 010601 (2016).

[6] A. D. Mirlin, Y. V. Fyodorov, F.-M. Dittes, J. Quezada, and T. H. Seligman, Phys. Rev. E **54**, 3221 (1996).

[7] Our notation is related to that in the literature by $\mu = \sigma = 2\alpha - 1 > 0$ and $\beta = b^{-\mu-1} > 0$.

[8] E. Cuevas, V. Gasparian, and M. Ortuno, Physical review letters **87**, 056601 (2001).

[9] L. Levitov, Annalen der Physik **8**, 697 (1999).

[10] A. D. Mirlin and F. Evers, Phys. Rev. B **62**, 7920 (2000).

[11] F. Evers and A. D. Mirlin, Rev. Mod. Phys. **80**, 1355 (2008).

[12] V. L. Quito, P. Titum, D. Pekker, and G. Refael, arXiv:1606.03094 (2016).

[13] O. Hallatschek and D. S. Fisher, Proceedings of the National Academy of Sciences **111**, E4911 (2014).

[14] S. Chatterjee and P. S Dey, Comm. Pure Appl. Math. **69**, 203 (2016).

[15] Supplementary Material recalls elementary properties of Q_{mn} , describes general properties of broad distributions and their self-averaging behaviour, discusses the mapping to epidemics model, and compares the BPBM to higher dimension Anderson models.

[16] P. Cizeau and J.-P. Bouchaud, Phys. Rev. E **50**, 1810 (1994).

[17] For BBRMs with $\mu < 0$, we observe also a rescaled semi-circle. This is expected, since [28] showed that the semi-circle law prevails for banded matrices with $\text{tr}(QQ^\dagger) \gg N$ as $N \rightarrow \infty$, which is indeed the case for $\mu < 0$.

[18] L. S. Schulman, J. Phys. A: Math. Gen. **16**, L639 (1983).

[19] M. Aizenman and C. M. Newman, Communications in Mathematical Physics **107**, 611 (1986).

[20] C. M. Newman and L. S. Schulman, Communications in Mathematical Physics **104**, 547 (1986).

[21] D. Coppersmith, D. Gamarnik, and M. Sviridenko, in *Proceedings of the thirteenth annual ACM-SIAM symposium on Discrete algorithms* (Society for Industrial and Applied Mathematics, 2002) pp. 329–337.

[22] M. Biskup, Random Structures & Algorithms **39**, 210 (2011).

[23] V. Oganesyan and D. A. Huse, Phys. Rev. B **75**, 155111 (2007).

[24] S. Ayadi, Random Operators and Stochastic Equations **17**, 1 (2009).

[25] S. Ayadi, Random Operators and Stochastic Equations **17**, 295 (2009).

[26] A. Rodríguez, V. Malyshev, G. Sierra, M. Martín-Delgado, J. Rodríguez-Laguna, and F. Domínguez-Adame, Phys. Rev. Lett. **90**, 027404 (2003).

[27] B. Altshuler, E. Cuevas, L. Ioffe, and V. Kravtsov, arXiv:1605.02295 (2016).

[28] M. Kuš, M. Lewenstein, and F. Haake, Phys. Rev. A **44**, 2800 (1991).

[29] J.-P. Bouchaud, L. F. Cugliandolo, J. Kurchan, and M. Mézard, Spin glasses and random fields **12** (1998).

[30] B. Derrida, Physical Review Letters **45**, 79 (1980).

[31] V. L. Nguyen, B. Z. Spivak, and B. I. Shklovskii, Sov. Phys.-JETP **62**, 1021 (1985).

[32] A. Gangopadhyay, V. Galitski, and M. Müller, Phys. Rev. Lett. **111**, 026801 (2013).

[33] F. Pietracaprina, V. Ros, and A. Scardicchio, Phys. Rev. B **93**, 054201 (2016).

[34] M. Kardar, G. Parisi, and Y.-C. Zhang, Physical Review Letters **56**, 889 (1986).

[35] E. Medina, M. Kardar, Y. Shapir, and X. R. Wang, Phys. Rev. Lett. **62**, 941 (1989).

[36] .

[37] A. M. Somoza, P. Le Doussal, and M. Ortuno, Phys. Rev. B **91**, 155413 (2015).

[38] M. Eden *et al.*, in *Proceedings of the Fourth Berkeley Symposium on Mathematical Statistics and Probability, Volume 4: Contributions to Biology and Problems of Medicine* (The Regents of the University of California, 1961).

[39] D. Richardson, Math. Proc. Cam. Phil. Soc. **74**, 515 (1973).

[40] R. Abou-Chacra, D. Thouless, and P. Anderson, Journal of Physics C: Solid State Physics **6**, 1734 (1973).

[41] R. Abou-Chacra and D. J. Thouless, Journal of Physics C: Solid State Physics **7**, 65 (1974).

SUPPLEMENTARY MATERIAL

The Supplementary Material is organised as follows. Sect. A recalls elementary properties of the distributions of Q_{mn} (Beta distribution). Sect. B discusses general properties of broad distribution. Sect. C discusses the self averaging property important for the block-diagonalisation argument in the main text. Sect D details the mapping between the matrix model and the epidemics model studied in [13, 14]. Sect. E discusses interpretation of the BBRM as a toy model to mimic the effect of higher dimension in the Anderson localisation; we will also discuss the important difference with Lévy matrix models [16]. Finally Sect. F provides further numerical evidence for the mobility edge.

A. Elementary properties of BBRM

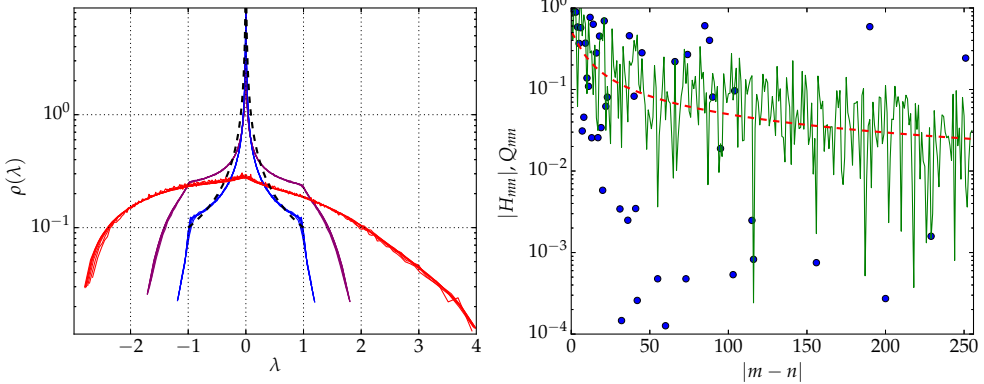


Figure 4. *Left*: Density of states of BBRMs, for $\mu = 0.5$, and $\beta = 1$ (red), 5 (purple) and 20 (blue, compared to the estimate (3), black), of matrix sizes $N = 2^{10} \dots 2^{14}$. The behaviour observed is representative of the DoS of BBRM for $\mu > 0$. *Right*: Snapshots of matrix elements of a BBRM (blue dots) and of a PBRM (green line), with $\mu = .5, \beta = 0.1$. The red dashed line depicts the standard deviation common to both.

The matrix element of BBRM Q_{mn} has a Beta distribution, which we recall here (see main text, Eq (2))

$$\mathbb{P}(Q_{mn} < q) = q^{1/g}, \quad g = \beta |m - n|^{\mu+1}, \quad q \in (0, 1). \quad (\text{A.1})$$

Note that the dependence on m, n and β is through g . Q_{mn} is uniformly distributed when $g = 1$ and $Q_{mn} \rightarrow 1$ becomes non-random as $g \rightarrow 0$; when $g \rightarrow \infty$ it becomes highly nontrivial. This justifies calling $\beta \rightarrow 0$ the *weak disorder* limit, and $\beta \rightarrow \infty$ the *strong disorder* limit consequently. The “clean” system limit $\beta = 0$ will not be considered because it is ill-behaving.

Its moments and Laplace transform are

$$\overline{Q_{mn}^k} = \frac{1}{1+kg} \stackrel{g \gg 1}{\sim} 1/(kg), \quad (\text{A.2})$$

$$\overline{\exp(-tQ_{mn})} = \sum_{k=0}^{\infty} \frac{(-t)^k}{k!} \frac{1}{1+kg} = g^{-1} t^{-1/g} (\Gamma(1/g) - \Gamma(1/g, t)). \quad (\text{A.3})$$

where $\Gamma(x, z) = \int_z^{+\infty} dy e^{-y} y^{x-1}$ is the incomplete Gamma function.

Q_{mn} can be characterised by the property that $-\ln Q_{mn}$ is exponentially distributed with mean value g :

$$\mathbb{P}(-\ln Q_{mn} > l) = \exp(-l/g), \quad l \geq 0. \quad (\text{A.4})$$

The typical value of Q_{mn} , which we define as the exponential of the mean of log, is

$$Q_{mn}^{\text{typ}} \stackrel{\text{def}}{=} \exp(\overline{\ln Q_{mn}}) = \exp(-g). \quad (\text{A.5})$$

As $g \rightarrow \infty$, $Q_{mn}^{\text{typ}} \ll \overline{Q_{mn}^k}$, see Eq (A.2). The same can be said about its median, which is $m(Q_{mn}) = \exp(-g \ln 2)$. Eq. (A) implies also that the occurrence probability of “black swans”

$$\mathbb{P}(Q_{mn} > a) \sim \frac{-\ln a}{g}, \quad g \rightarrow \infty, 0 < a < 1 \text{ fixed.} \quad (\text{A.6})$$

In numerical simulations, the matrix elements are generated as $Q_{mn} = u^g$, where $u \in [0, 1]$ is uniformly distributed. In Fig. 4 (right), a sample of the BBRM, as function of $|m - n|$, is compared to PBRM with the same parameters.

As argued in the main text, Eq. (3), when $\mu > 0, \beta \gg 1$, the density of states of the BBRM is essentially that of $\pm Q_{01}$. In Figure 4 (left), we show a numerical check of this claim. We observe also that even for $\beta \sim 1$, the density of states of BBRM differs significantly from the semicircle law.

B. Broad distribution in general

We advocated in the text that the following criterion on the matrix element distributions to be *broadly distributed*

$$\overline{Q_{mn}^k} \stackrel{g \gg 1}{\sim} c(k)/g \Leftrightarrow \overline{e^{-tQ_{mn}}} = 1 - f(t)/g + O(g^2), \quad g \rightarrow \infty. \quad (\text{B.1})$$

where $f(t) = \sum_{k>0} (-1)^{k-1} c(k) t^k / k!$ is independent of g . BBRM satisfies this criterion since by (A.1),

$$f_{\mathbf{B}}(t) = \log(t) + \Gamma(0, t) + \gamma_E, \quad c(k) = 1/k. \quad (\text{B.2})$$

where $\gamma_E = 0.57\dots$ is the Euler constant. What can we say about a generic distribution satisfying Eq (B.1)? What additional properties are needed in order to justify the name “broadly distributed”? The rest of this subsection discusses these questions. For this we assume that $Q = Q_{mn} \geq 0$ (if this is not the case, replace Q by $|Q|$ below). Then the Laplace transform of Q can be written as the cumulative distribution of $\log Q$ convoluted with a variable G drawn from a standard Gumbel distribution:

$$\overline{\exp -tQ} = \overline{\exp(-\exp(\ln Q + \ln t))} = \overline{\theta(-\ln Q - G - \ln t)} = \mathbb{P}(-\ln Q - G > \ln t) \quad (\text{B.3})$$

here G and $\log Q$ are independent, and $\theta(x)$ is the Heaviside step function. Now $\overline{\exp -tQ} = 1 - f(t)/g + O(1/g^2)$ implies (we denote $y = \ln t$)

$$\mathbb{P}(-\ln Q - G > y) = 1 - f(e^y)/g + O(1/g^2). \quad (\text{B.4})$$

By setting $y = 0$ we have $\mathbb{P}(\ln Q + G > 0) = f(1)/g$. Since $G \sim O(1)$, this implies $Q \sim O(1)$ with probability $\propto 1/g$, in agreement with (A.6).

The typical magnitude of Q^{typ} can be estimated by the value y for which the cumulative $\mathbb{P}(-\ln Q - G > y)$ is smaller than 1, namely when $f(e^y) \sim g$. This gives $-\ln Q \sim y \sim \ln f^{\text{inv}}(g)$ and

$$Q^{\text{typ}} \sim 1/f^{\text{inv}}(g) \quad (\text{B.5})$$

where f^{inv} is the inverse function of f . Now, for BBRM, Eq (B.2) implies that $f_{\mathbf{B}}(t \rightarrow +\infty) \sim \ln t$ for t large, so $Q^{\text{typ}} \sim 1/f_{\mathbf{B}}^{\text{inv}}(g) \sim \exp(-g)$, in agreement with Eq. (B.5). This exponential typical value decay depends only on the logarithmic asymptotic growth of $f(t \rightarrow +\infty)$, not on its precise form. In what follows, we will assume, in addition to (B.1), that $f(t)$ grows at most logarithmically

$$f(t \rightarrow +\infty) \lesssim c \ln t. \quad (\text{B.6})$$

This condition will be useful in Sect. C 2, and is not very restrictive. For example, besides BBRM, it is satisfied by randomised long-range percolation graph Hamiltonians (see main text for definition). Indeed, in this case, we have $\overline{\exp(-t|Q|)} = 1 - (1 - \overline{\exp(-t|H|)})/g$ where H is a fixed distribution, so $f(t) = 1 - \overline{\exp(-t|H|)} \leq 1 \ll \ln t$ as $t \rightarrow +\infty$.

In summary, under the condition (B.1) and a mild technical condition (B.6), we can recover all characteristics that justify the name “broadly distributed”. Therefore, we expect that any banded random matrix model whose entries fall in this class has localisation transition in the $\mu \in (0, 1)$ regime. We note however two subtle points. First, the shape of density of state is dependent on the distribution of Q_{mn} for $|n - m|$ small. Second, the existence of mobility edge in the $\beta \gg 1$ limit relies crucially on the absence of diagonal disorder; if we add an Anderson-model type diagonal disorder of fixed width to BBRM, we observe a critical β_c for which all states are localised when $\beta > \beta_c$.

C. Self-averaging property

In the next section C, we will discuss the statistical property of sums of matrix elements, on which the block-diagonalisation procedure of the main text is based. Our arguments are valid for general broadly distributed matrix models, and the BBRM will serve as a concrete example.

As we have seen, for broadly distributed Q_{mn} , the typical value is very small compared to its moments when $g = \beta |m - n|^{\mu+1}$ is large. On the other hand, since all moments exist, for any fixed g , the central limit theorem applies and the sum of M independent copies of Q_{mn} tends to a Gaussian as $M \rightarrow \infty$. How large should M be, in function of g , so that the the sum becomes narrow distributed? It turns out that $M \geq g$ is sufficient (and necessary). Intuitively, this condition ensures that the rare event $Q_{mn} \sim O(1)$ does occur in the sum, Eq (A.6). In subsection C 1 we derive this result and in subsection C 2, we extend it to the case of sums with random coefficients, needed to estimate the sum of Eq.(5) of the main text.

1. Sum without coefficient

Let Q_i, \dots, Q_M denote M independent identical copies of Q_{mn} , with $g = \beta |m - n|^{\mu+1}$, and S their sum:

$$S \stackrel{\text{def}}{=} \sum_{i=1}^M Q_i. \quad (\text{C.1})$$

The distribution of S has a well-defined limit S_T when $M, g \rightarrow \infty$ with $M/g = T$ kept constant. For this, all we need is the expansion $\overline{\exp(-tQ_{mn})} = 1 - f(t)/g + O(1/g^2)$, Eq. (B.1), which is valid for general broad distribution. Combined with Eq. (C.1), we have:

$$\overline{\exp(-tS)} = \left[\overline{\exp(-tQ_{mn})} \right]^M \longrightarrow \exp(-Tf(t)), \quad M = Tg \rightarrow \infty. \quad (\text{C.2})$$

So, the distribution of S has a limit S_T depending on T , given in terms of Laplace transform

$$\overline{\exp(-tS_T)} = \exp(-Tf(t)). \quad (\text{C.3})$$

For BBRM, by (B.2), the cumulants of S_T have a simple form:

$$\overline{S_T^k}^c = (-1)^{k-1} T \frac{d^k f}{dt^k}(0) = T/k. \quad (\text{C.4})$$

From (C.2) we conclude that when $M \sim g$, the distribution of the sum is g -independent in the $g \rightarrow \infty$ limit. Therefore, when $M \gg g$, we enter the central limit theorem regime, in which $S \sim \sqrt{M/g}$ typically. On the other hand, when $M \ll g$, $T \ll 1$, (C.3) implies $\overline{\exp(-tS_T)} \sim 1 - Tf(t) + O(T^2)$, so the sum S_T becomes itself broadly distributed, with $1/T$ playing the rôle of g .

It is interesting to note that, in the case of BBRM, the sum S is nothing but the partition function of a exponential random energy model (such models are relevant for modeling glassy dynamics [29]). The model is defined by M independent energy levels E_i which are exponentially distributed with mean $\overline{E_i} = M$. Note that Q_i has the same distribution as the Boltzmann factor $\exp(-E_i/T)$ at temperature T . So the partition function $Z = \sum_{i=1}^M \exp(-E_i/T)$ has the same distribution as S . In this respect, Eq. C.2 and (C.3) calculated the partition function distribution in the thermodynamic $M \rightarrow \infty$ limit. Remarkably, in that limit, $Z \sim O(1)$ at any temperature. In consequence, the entropy $\sim O(1)$ as well; *i.e.*, the model is always in the low temperature phase, where a few Boltzmann weights dominate Z (to compare, the well-known Gaussian random energy model [30] has a transition to the high temperature phase).

Having treated the simplest case in some detail, we come to the extensions we needed in the text, focusing on the case $M = g$.

2. Sum with coefficient

In the previous subsection we dealt with the sum of independent Q_{mn} . A key quantity of our block-renormalisation argument is the transformed matrix element

$$\tilde{Q} \stackrel{\text{def}}{=} \tilde{Q}_{\alpha\gamma}^{(k)} = \sum_{m,n} Q_{mn} v_{mn}, \quad v_{mn} = \langle \phi_{\alpha}^{(k)} | m \rangle \langle n | \phi_{\gamma}^{(k)} \rangle, \quad (\text{C.5})$$

see Eq. (5) of main text. Recall that in the sum, n and m range over two blocks of size $\ell_k \sim M^{\frac{1}{2}}$, and separated by a distance $\ell_{k+1} \sim M^{2/(\mu+1)}$ such that $\beta \ell_{k+1}^{\mu+1} = g = M$. Since $\ell_k \ll \ell_{k+1}$, all the Q_{mn} 's have approximately the same distribution as Q_i in (C.1). However, In the two cases discussed in the text, the coefficients v_{mn} behave quite differently, so we treat them separately below.

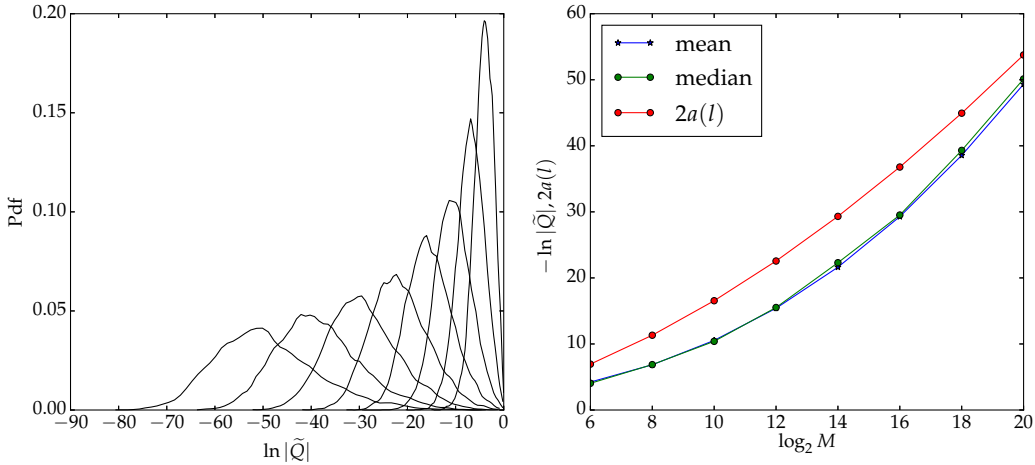


Figure 5. Left: Histogram of $\ln |\tilde{Q}|$ with $v_{mn} = \pm \exp(-a(m) - a(n))$ with random independent signs and $a(m) = \ln^\kappa(m)$, $\kappa = 1.7$, from $M = 2^6$ (rightmost) to $M = 2^{20}$ (leftmost). Right: The mean and median of $\ln |\tilde{Q}|$, compared to the prediction $2a(l)$.

a. Extended case. v_{mn} are all identically distributed as v_{GOE}/ℓ_k where v_{GOE} is a fixed narrow distribution (*i.e.*, the independent product of two GOE envelope amplitudes times square root of the matrix size). Although they are not independent, their correlation is weak and we can safely assume the following mixing property: for M large, the number of v_{mn} in any interval $[x/\ell_k, y/\ell_k]$ can be approximated by $M \int_x^y \rho(v)dv$, where ρ is the probability density function of v_{GOE} . Then it is not hard to obtain

$$\overline{\exp(-t\tilde{Q})} \xrightarrow{M=g \rightarrow \infty} \exp(-f_1(t/\ell_k)), \quad f_1(s) = \int f(tv)\rho(v)dv. \quad (\text{C.6})$$

As claimed in the text, we conclude that the transformed matrix element $\tilde{Q}_{\alpha\gamma}^{(k)}$ behaves as a narrowly distributed random variable of order $1/\ell_k$.

b. Localised case. $v_{mn} = \langle \phi_\alpha | n \rangle \langle m | \phi_\gamma \rangle$ are the products of two amplitudes of localised eigenstates that decays as $\langle \phi_\alpha | n \rangle \sim \pm \exp(-a(|n - n_\gamma|))$ in large but finite systems $|n - n_\gamma|, |m - m_\alpha| \leq \ell = \ell_k = M^{1/2}$; the notation here is related to that in main text by $a(\ell_k) = a_k$. This implies that the empirical distribution of (v_{mn}) is also broad, making the current case more involved. Below, we shall argue that, *under the condition* (B.6), $\tilde{Q}^{\text{typ}} \sim e^{-2a(\ell)}$, as claimed in the text.

For this, let us consider two (extremal) types of contributions to the sum (C.5). (i) For the terms $m, n \sim 1$, $v_i \sim 1$; since there are only $O(1)$ such terms, black swans in Q_{nm} cannot occur (except in rare events of probability $\sim 1/M$), so we have $Q_{nm} \sim Q^{\text{typ}}$, and the total contribution of these terms is I $\sim Q^{\text{typ}}$. (ii) For the terms $m, n \sim \ell$, $v_{mn} \sim e^{-2a(\ell)}$; since there are $\sim M$ of them, there will be $O(1)$ black swans $Q_{nm} \sim 1$, so the total contribution is II $\sim e^{-2a(\ell)}$. Now, under the condition (B.6), we have $Q^{\text{typ}} \sim e^{-g} = e^{-\ell^2}$ by (B.5); on the other hand, since $e^{-a(\ell)}$ is the decay rate of a localised eigenstate, $e^{-2a(\ell)} \gg e^{-\ell^2}$ in any case. Therefore II \gg I, thus we conclude that the contribution I dominates \tilde{Q} , and $\tilde{Q} \sim e^{-2a(\ell)}$, as desired. A more quantitative argument is provided in Appendix 1.

We end this discussion with the numerical results of Figure 5. In the left panel we plot histograms of $S[v_i]$ as defined in (1.1) (we have checked that the results is insensitive to the presence of random signs). We see that the distribution $\ln |S[v_i]|$ broadens as $M = \ell^2$ grows. Thus, compared to the extended case (see (C.6)), the magnitude of $\tilde{Q}_{\alpha\gamma}^{(k)}$ in the localised case fluctuates much more around its typical value. This strong fluctuation, combined with strong finite size effects, makes the prediction of the decay rate of localised eigenstate in $\mu \in (0, 1)$ regime hard to access numerically.

D. Mapping to epidemics model

The long-range epidemics model mentioned in the main text [13, 14] is a long-range first passage percolation (FPP) model. This section describes the relation between this model and BBRM, through a mapping that involves another statistical mechanics model, that of undirected, long-range “polymers” in random media, see Figure 6.

We begin by recalling the FPP model (its relation with the growth/epidemics model will be discussed below). For this, one considers a symmetric matrix of independent random waiting times (energies) τ_{mn} having exponential

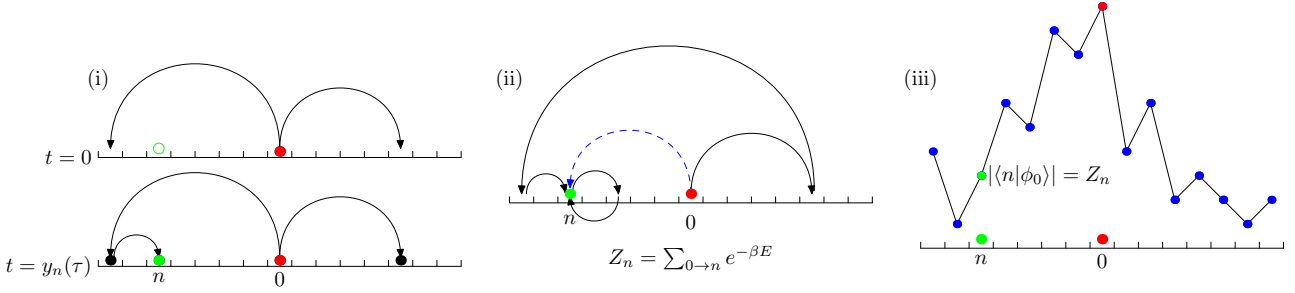


Figure 6. Illustration of models involved in the mapping described in Sect. D. (i) In the growth/epidemics model, occupied sites send offspring to empty sites at a rate $\ell^{-\mu-1}dt$, where ℓ is the source-destination distance; two snapshots of the system, at $t = 0$ and $t = T_n(\tau)$ (moment at which the site n is infected) are depicted here. (ii) In the polymer model, which is a finite temperature extension of the growth model, we sum over all paths connecting two points 0 and n , ranging from the direct path (blue, dashed) and detoured paths with loops, for example, the one in black. (iii): The amplitude at site n of (strong-disorder) BBRM eigenstates localised around 0 is in turn related to the polymer partition function by (D.10).

distribution:

$$\tau_{nn} \equiv +\infty, \mathbb{P}(\tau_{m \neq n} > \tau \geq 0) = \exp - \frac{\tau}{|m - n|^{\mu+1}}, \quad (\text{D.1})$$

A key quantity in FPP models is the *first-passage time*, of which we review the definition here. For this, let us call a *path* between two points 0 and m any finite sequence of sites $\mathbf{p} = (0 = m_0, m_1, \dots, m_s = n)$, s being its length. Note that paths are not directed and sites can be visited multiple times. The total waiting time (energy) of a path is defined as the sum

$$T[\mathbf{p}] = \sum_{i=1}^s (\tau_{m_i, m_{i-1}} - \tau), \quad (\text{D.2})$$

where τ is a fixed cost ($T[\mathbf{p}]$ has nothing to do with the T in Sect. C1). Then the first passage time is defined by taking the minimum among all paths connecting two points:

$$T_n(\tau) \stackrel{\text{def}}{=} \min_{\mathbf{p}: 0 \rightarrow n} T[\mathbf{p}]. \quad (\text{D.3})$$

Note that when $\tau \leq 0$, the minimum cost is not changed if one restricts to *simple* paths, *i.e.*, those visiting no site more than once. Yet, when $\tau > 0$, there could be some $\tau_{mn} < \tau$, $a_{mn}(\tau) = -\infty$ in (D.3), because going back and forth $m \leftrightarrow n$ *ad infinitum* lowers arbitrarily the energy. We will discuss its significance for delocalisation in the end of this section.

We know that Q_{mn} (A.1) has the same distribution as the matrix of Boltzmann factors ($e^{-\beta\tau_{mn}}$) at temperature $1/\beta$ (D.1). This allows us to extend the FPP to a finite temperature statistical physics model, of which the partition function at temperature β^{-1} is simply

$$Z_n(\lambda) = \sum_{\mathbf{p}: 0 \rightarrow n} \exp(-\beta T[\mathbf{p}]) = \sum_{s=0}^{\infty} \sum_{m_1} \dots \sum_{m_{s-1}} \prod_{i=1}^s (Q_{m_i m_{i-1}} \lambda^{-1}), \quad \lambda = e^{-\beta\tau}. \quad (\text{D.4})$$

To wit, $Z_n(\lambda)$ is the sum over all paths with endpoints 0 and n of Boltzmann factors with energy $T[\mathbf{p}]$ (D.2), and λ^{-1} (τ) is the fugacity (chemical potential, respectively) coupled to the path length. This sum does not diverge only when $\lambda \geq 1 \Leftrightarrow \tau \leq 0$. It can be seen as the partition function of a model of “polymers” in random media, where the polymers are *undirected* and the monomers can stretch over arbitrarily long distance. We draw a few such polymer configurations is given in Figure 6 (ii). By construction, we have the following zero temperature limit of the free energy:

$$-\frac{1}{\beta} \ln Z_n(\lambda) \xrightarrow{\beta \rightarrow \infty} T_n(\tau), \quad (\text{D.5})$$

whenever $-\frac{1}{\beta} \ln \lambda \xrightarrow{\beta \rightarrow \infty} \tau$.

We show now that how $T_n(\tau)$ grows with $|n|$ is related to the decay of eigenstates in the $\beta \gg 1$ regime. For this, it suffices to observe from Eq. (D.4) that $Z_n(\lambda)/\lambda$ is the matrix product expansion of the resolvent of \mathbf{Q} :

$$Z_n(\lambda)/\lambda = \sum_{s=0}^{+\infty} \lambda^{-s-1} \langle n | \mathbf{Q}^s | 0 \rangle = \langle n | (\lambda \mathbf{I} - \mathbf{Q})^{-1} | 0 \rangle, \quad (\text{D.6})$$

so by (D.5) we have

$$\ln \langle n | (\lambda \mathbf{I} - \mathbf{Q})^{-1} | 0 \rangle \stackrel{\beta \gg 1}{\approx} \beta T_n(\tau), \quad (\text{D.7})$$

which is just Eq. (9) of the main text. The relation between the decay of resolvent and that of eigenstates is quite standard, as we briefly review now for the Reader's convenience. For this, we expand the resolvent over all the eigenstates $|\lambda'\rangle$ of \mathbf{Q} (with energy λ'), we

$$\langle n | (\lambda \mathbf{I} - \mathbf{Q})^{-1} | 0 \rangle = \sum_{\lambda'} \frac{\langle n | \lambda' \rangle \langle \lambda' | 0 \rangle}{\lambda - \lambda'}. \quad (\text{D.8})$$

Because of the denominator, the sum is dominated by eigenstates with energy close to λ , and the decay of those eigenstates determines the behavior $\langle n | \lambda' \rangle \langle \lambda' | 0 \rangle$ as a function of n . Indeed, when $|\lambda'|$ is localised around some site m with decay $\ln |\langle n | \lambda' \rangle| = -a(|m - n|)$, we have $\ln |\langle n | \lambda' \rangle \langle \lambda' | 0 \rangle| = -a(|m|) - a(|n - m|) \leq -a(|n|)$ (since $a(n)$ is always linear or sub-linear), so the eigenstates localised at 0 or n will dominate (D.8) and give the same contribution:

$$\ln |\langle n | (\lambda \mathbf{I} - \mathbf{Q})^{-1} | 0 \rangle| \approx \ln |\langle n | \phi_0 \rangle|, \quad (\text{D.9})$$

where $|\phi_0\rangle$ is an eigenstate localised around 0 having energy $\approx \lambda$. Combined with (D.7), we have

$$-\ln |\langle n | \phi_0(\lambda) \rangle| \stackrel{\beta \gg 1}{\approx} \beta T_n(\tau). \quad (\text{D.10})$$

If $T_n(\tau)$ does not increase with $|n|$, the state $|\phi_0\rangle$ in fact extended. Note that since $\lambda = e^{-\beta\tau}$ (Eq. (D.4)), when $\beta \gg 1$, any λ that is not exponentially large or small will corresponds to $|\tau| \sim \beta^{-1} \rightarrow 0$. So Eq. (D.10) and (D.7) relate $T_n(0)$ to the whole spectrum save an exponentially small vicinity of $\lambda = 0$.

We remark that the mapping above is a new instance of the well-known interplay between polymer in random media and localisation [5, 31–33], a highlight of which has been relating the conductance fluctuations in short-range Anderson model to Kardar-Parisi-Zhang (KPZ) [34] universality class [35–37].

Now we discuss the relation to growth/epidemics models. It is well known that KPZ class describes not only directed polymers in random media, but also stochastic non-equilibrium surface growth. In fact, thanks to the exponential waiting time (D.1) the above long range FPP model is also a growth/epidemics model, whose dynamics is described as follows (see Figure 6 (i)): the sites are occupied or empty, and any occupied site m stays so and sends offspring to any clean site n with rate $d\mathbb{P} = |m - n|^{-\mu-1} dt$, and newly infected sites wait $-\tau$ before being able to infect others. The initial condition is that only one site 0 is newly infected at $t = 0$. Then, it is not hard to see that $T_n(\tau)$ (D.3) has the same distribution as the moment when the site n is infected.

The short-ranged version of such growth model has been proposed long ago [38, 39]. In this case, the first passage time is proportional to the distance in any spatial dimensions, which corresponds, via (D.10), to the exponential decay of wave-functions in the Anderson model (in the localised phase). The fluctuations of T_n are believed to belong to the KPZ universality class, which also governs the log-conductance fluctuations of the Anderson's model in the insulator phase [36]. In the long-range first passage percolation model the leading behavior of $T_n(\tau = 0)$ is much richer; its non-trivial dependence on μ has been revealed by [13, 14]. Their results and translation by (D.10) are summarised in the Table I.

To end this section, we comment the case $\tau > 0$, corresponding (see (D.5)) to energy λ exponentially close to 0 as $\beta \rightarrow \infty$ ($\tau < 0$ is unphysical: there are no eigenstates with exponentially large energy). As we observed above, the formal partition sum (D.4) diverges and ground state energy (D.3) collapses to $-\infty$ when there are links (m, n) for which

$$Q_{mn} > \lambda = e^{-\beta\tau} \Leftrightarrow \tau_{mn} < \tau, \quad (\text{D.11})$$

since $Q_{mn} = e^{-\beta\tau_{mn}}$. When the above condition is satisfied, one has the divergence of $\sum_{k=0}^{\infty} Q_{mn}^{2k}/\lambda^{2k}$, which is the contribution of repeatedly going back and forth $m \leftrightarrow n$ to partition function (D.4). From the polymer statistical mechanics point of view, at the onset of divergence $Q_{mn} = \lambda - \varepsilon$, the polymer tends to *condensate* (occupy infinite

$\mu \in$	$T_n(0) \propto$	BBRM $ \langle n \phi_0 \rangle \sim$	PBRM $ \langle n \phi_0 \rangle \sim$
$(-1, 0]$	$\xrightarrow{L \rightarrow \infty} 0$	extended	extended
$(0, 1)$	$(\ln n)^{\kappa(\mu)}$	$\exp(-c \ln^{\kappa(\mu)} n)/\text{extended}$	extended
$\{1\}$	$e^{c\sqrt{\ln n }}$	$\exp(-e^{c\sqrt{\ln n }}) / \text{extended}$	critical
$(1, 2)$	$ n ^{\mu-1}$	$\exp(-c n ^{\mu-1})$	$ n ^{-(\mu+1)/2}$
$(2, \infty)$	$ n $	$\exp(-c n)$	$ n ^{-(\mu+1)/2}$

Table I. Summary of asymptotic first-passage time [13, 14] of the first-passage percolation model and their implication on the eigenstate decay of BBRM. $\kappa(\mu) = \ln 2 / \ln \frac{2}{\mu+1}$. The results on PBRM [6] are also shown to compare. All the results are discussed in the main text, except the regime $-1 < \mu < 0$. There, $a_n(0) \rightarrow 0$ in the $L \rightarrow \infty$ limit. By (D.10), this means the eigenstates are extended even in the $\beta \gg 1$ limit. The spontaneous growth abolishes the notion of distance and makes BBRM equivalent to GOE when $\mu < 0$.

number of times) on the link $m \leftrightarrow n$. Beyond that point, the statistical mechanics model is unphysical. However, from the quantum mechanics (matrix eigenstates) point of view (Eq. (D.10)), such divergence should be re-summed and interpreted as *resonance* between sites m and n . From (D.1) and (D.11), one sees that the probability of such resonance is $P_{nm} = 1 - e^{-\tau/|n-m|^{\mu+1}}$, as claimed in the main text. There we argued that the eigenstate will de-localise when the network formed by connecting resonating sites percolates the whole system. The above discussion suggests thus a correspondence between (de)-localisation transition and proliferation of polymer condensation; detailed study of this point will be undertaken in a future work.

E. Comparing with higher dimension

In Anderson models on short-range lattices, the localised eigenstates decays always exponentially in function of the distance: $|\langle \phi_m | n \rangle| = \exp(-D(m, n)/\xi)$ where $D(m, n)$ is the distance between sites m and n on the lattice. Let us define $N(y)$ as the number of sites n on which the amplitude $|\langle \phi_m | n \rangle| > e^{-y}$ is large. This is equal the number of pair inside the domain with $D(m, n) < \xi y$. In finite dimension we have

$$N(y) = Cy^d, \quad (\text{E.1})$$

where C is a constant. On a Cayley tree with degree $K+1$, we have

$$N(y) = C \exp(K\xi y). \quad (\text{E.2})$$

so Anderson models on trees are regarded as $d = \infty$ models.

In this respect, we can interpret BBRM to higher dimensional (short-range) model by computing $N(y)$ using results of Table I. For this, note that by (9), $N(y) = l$ is equivalent to $y_l = y$. So we just need to inverse the function T_n .

- $\mu \geq 2 \Rightarrow N(y) = y$, giving an effective dimension $d = 1$.
- $\mu \in (1, 2) \Rightarrow N(y) = y^{1/(\mu-1)}$, giving an effective dimension $d = 1/(\mu-1)$. As $\mu \searrow 1$, $d \nearrow \infty$.
- $\mu \in (0, 1) \Rightarrow N(y) = \exp(y^{1/\kappa})$, with $\kappa > 1$: $N(y)$ grows faster than any finite dimension (Eq. (E.1)), but slower than Cayley tree (Eq. (E.2)). So the localisation transition and mobility edge in this regime is distinct from those in other mean-field models, such as Anderson model on Cayley trees [40, 41] and the model of Lévy matrices [16]. A remarkable property of the latter is that the mobility edge can be exactly calculated [5]. This is not plausible for our model, since as we can see in the block-renormalisation process, whether the system flows to the extended or localised phase depends on the first a few steps of iteration, thus on the microscopic details of the model. Nevertheless, the renormalisation group method give access to critical properties of the localisation transition fixed points. Results on this direction will be reported elsewhere.

F. Further numerics on the existence of mobility edge

The analytical arguments of the main text show that for $\mu \in (0, 1)$, and for a given energy λ , the eigenstate is localised when $\beta \gg 1$ and extended when $\beta \ll 1$. *A priori*, this implies that there are two possible scenarios:

- i There is a unique value β_c , such that for $\beta > \beta_c$ ($\beta < \beta_c$), all the eigenstates are localised (extended, respectively). If this were the case, there would be no mobility edge.
- ii The critical disorder $\beta_c = \beta_c(\lambda)$ depends on the energy λ non-trivially. In this case, mobility edge exists at least for some β .

The Figure 3 (b) of the main text shows already that mobility edges exist, *i.e.*, the possibility ii holds. Here, we provide further numerical evidence to rule out completely the alternative possibility. In Figure 7, we show a zoom-in of Figure 3 (a) to the near-critical regime. We observe that the critical value β_c depends clearly on energy λ , going from $\beta_c(0.7 < \lambda < 0.9) \approx 5.8$ to $\beta_c(1.1 < \lambda < 1.3) \approx 5.2$. Moreover, we remark that the critical value of the rescaled gap ratio $\chi_c \approx .28(2)$ is independent of λ ; this indicates that for a given $\mu \in (0, 1)$, there is one unique critical point of localisation transition.

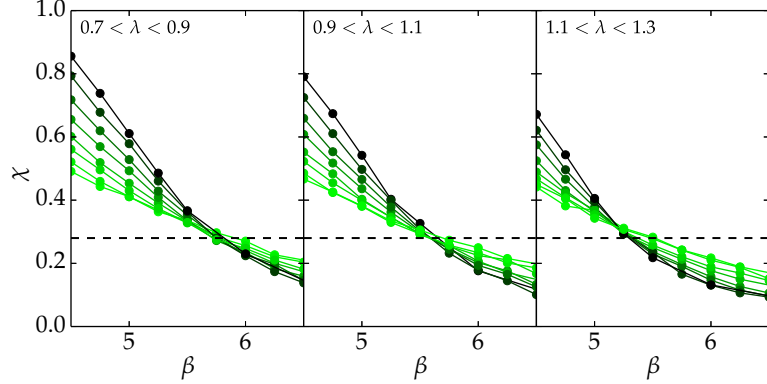


Figure 7. A zoom-in to the critical regime of Fig. 3 (a) of main text. We locate the critical value of the rescaled gap ratio observable $\chi_c \approx .28(2)$. Note also that the location of the transition β_c varies in $\in (5, 6)$ as a function the energy $\lambda \in (.7, 1.3)$; this implies that at least for the above range of β , the matrix model has a mobility edge at $\lambda \in (.7, 1.3)$.

1. Appendix: another estimate of \tilde{Q} in the localised case

Here we use the method of eqs. (B.4) and (B.5) to estimate Q^{typ} . For this, we shall assume $Q_{nm} \geq 0$ and approximate the amplitudes $\langle \phi_\alpha | n \rangle$ with their decay $\exp(-a(n))$, neglecting fluctuations and signs. Then we can show that

$$\overline{\exp(-t\tilde{Q})} \approx \exp \left[- \sum_{m,n=1}^{\ell} f \left(t e^{-a(m)-a(n)} \right) / \ell^2 \right]. \quad (1.1)$$

Since $\tilde{Q} \geq 0$ in this approximation, we have similarly to (B.4)

$$\mathbb{P}(\ln \tilde{Q} + G < -\ln t) = \overline{\exp(-t\tilde{Q})} = \exp \left[- \sum_{m,n=1}^{\ell} f \left(t e^{-a(m)-a(n)} \right) / \ell^2 \right], \quad (1.2)$$

where G is an independent standard Gumbel variable, negligible compared to $-\ln \tilde{Q}$. So we can define the typical value $s = \tilde{Q}^{\text{typ}}$ by the criterion

$$\mathbb{P}(\ln \tilde{Q} + G < \ln s) = e^{-1}. \quad (1.3)$$

Combined with (1.2) this gives the following implicit equation for s :

$$F(s) \stackrel{\text{def}}{=} \sum_{m,n=1}^{\ell} f \left(e^{-a(m)-a(n)} / s \right) / \ell^2 = 1. \quad (1.4)$$

In the main text, we claimed that the solution to this equation is $s \sim e^{-2a(\ell)}$ asymptotically, which we show now, by arguing that (i) $s \gtrsim e^{-2a(\ell)}$ and (ii) $s \lesssim e^{-2a(\ell)}$. For this let us recall that the assumption $Q \geq 0$ implies $f(t)/g = -\ln \overline{e^{-t\tilde{Q}}} + O(1/g^2)$ (B.1) is an increasing function of t , and thus the $F(s)$ decreases as s increases.

(i) Let $s_{\inf} = e^{-2a(\ell)} f^{\text{inv}}(1)$, so that $\exp(-a(m) - a(n))/s_{\inf} \geq f^{\text{inv}}(1)$, so

$$F(s_{\inf}) \geq \sum_{m,n=1}^{\ell} 1/\ell^2 = 1 = F(s) \Rightarrow s \geq s_{\inf} \sim e^{-2a(\ell)}.$$

(ii) Here we shall need the assumption $f(t \rightarrow +\infty) \leq c \ln t$, Eq. (B.6). This implies the estimate

$$1 = F(s) \leq -\frac{c}{\ell^2} \sum_{m,n=1}^{\ell} (a(m) + a(n) + \ln s) = -c \ln s - \frac{2c}{\ell} \sum_{n=1}^{\ell} a(n) \Rightarrow \ln s \leq -c^{-1} - \frac{2}{\ell} \sum_{n=1}^{\ell} a(n) \sim -2a(\ell) - c^{-1},$$

where the last estimate holds for a large class of growth $a(n)$, including $a(n) \propto \ln^{\kappa}(n/\xi)$, $\kappa > 1$, of the main text. Thus we have $s \lesssim e^{-2a(\ell)}$ as desired.

Combining the two estimates, we conclude that $\tilde{Q}^{\text{typ}} = s \sim e^{-2a(\ell)}$, as claimed in the text.